Structural Studies on Layered Alkylpyridinium Iodopalladate Networks

Francesco Neve,*,† Alessandra Crispini,† and Oriano Francescangeli‡

Dipartimento di Chimica, Università della Calabria, 87030 Arcavacata di Rende (CS), Italy, and Dipartimento di Scienze dei Materiali e della Terra, Sezione Fisica, Università di Ancona, Via Brecce Bianche, 60131 Ancona, Italy

Received June 15, 1999

The reaction of alkylpyridinium ($C_nH_{2n+1}NC_5H_5$, hereafter C*n*-Py) iodide salts in aqueous acetonitrile with a preformed palladium iodide precursor afforded two different types of organic−inorganic phases depending on the molar ratio. A 2:1 ratio yielded the phase $[Cn\text{-Py}]_2[PdI_4]$ (**3**, $n = 14$, 16), which crystallized in the triclinic crystal system. The X-ray crystal structure of **3**, ($n = 14$), refined in the space group $P\bar{1}$ ($a = 8.918(3)$ Å, $b = 9.894(3)$ Å, $c = 29.062(12)$ Å, $\alpha = 93.51(3)°$, $\beta = 94.17(3)°$, $\gamma = 115.60(3)°$, and $Z = 2$), consists of interdigitated bilayers with a basal spacing of 29.0 Å. The aliphatic chains of the cations, which run almost parallel to the stacking direction, are fully stretched between polar planes built on isolated $[PdI_4]^{2-}$ anions and cation headgroups. Changing the organic cation to palladium ratio to 1:1 led to a new phase $[Cn\text{-Py}]_2[Pd_2I_6]$ (**4**, $n = 14$, 16), which crystallizes in the triclinic $P\bar{1}$ space group ($a = 9.399(4)$ Å, $b = 14.264(6)$ Å, $c = 29.415(13)$ Å, $\alpha = 92.11(4)°$, $\beta = 90.07(4)°$, $\gamma = 104.53(3)°$, $Z = 3$ for **4**($n = 14$); $a = 9.417(2)$ Å, $b = 14.215(3)$ Å, $c = 31.552(6)$ Å, $\alpha = 87.96(3)°$, $\beta = 87.63(3)°$, $\gamma = 75.67(3)°$, $Z = 3$ for **4**($n = 16$)). The layered structure is basically of a continuously interdigitated single-layer type, with a bilayer sublattice superimposed. Isolated $[Pd_2I_6]^{2-}$ anions contribute to the inorganic planes. A high degree of interdigitation and tilting of the aliphatic chains lead to basal spacings of 29.4 and 31.5 Å for **4**($n = 14$) and **4**($n = 16$), respectively. The $[Cn\text{-Py}]_2[PdI_4]$ and $[Cn\text{-Py}]_2[Pd_2I_6]$ phases were characterized by thermal analysis. Mesomorphic behavior was observed only for **3**($n = 16$), which was confirmed by variable-temperature powder XRD and optical microscopy.

Introduction

Organic−inorganic mesoscopic materials are being currently investigated because of the intriguing possibility of combining the features of both inorganic and organic systems within a single material.[1−7] Due to the nature (molecular, ionic, hydrogen-bonding, etc.) of the organic and inorganic components many different combinations may be achieved. The alternate variation of each component may then lead to a practically endless modulation of the shape, rigidity, and functionality of the composites.

Low-dimensional organic−inorganic compounds based on inorganic anions and organic cations have created a wide interest and are being studied as two-component,[8−14] or multicomponent[15,16] hybrid materials with the aim of controlling their organization (and functionalities) in the solid state. Recently, we contributed to the field through the preparation of two series of compounds based on *N*-alkylpyridinium ($C_nH_{2n+1}NC_5H_5$, hereafter C*n*-Py) cations and tetrahalopalladate anions.[17] The compounds, $[Cn\text{-Py}]_2[PdX_4]$ (**1** (X = Cl), **2** (X = Br); $n = 12$, 14, 16, and 18), crystallized as layered solids with a continuously interdigitated "brick architecture"[18,19] (layering motif **A** in Chart 1) and exhibited thermotropic liquid-crystalline behavior.[17] The latter had smectic character, a natural consequence of the solid-

Chart 1

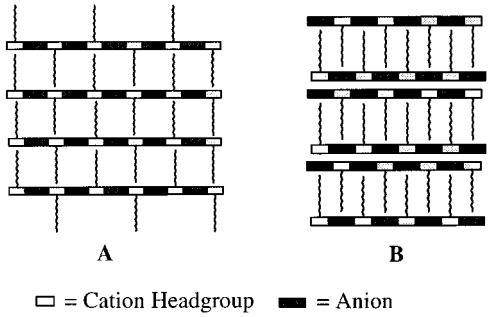

* Corresponding author. Fax: +39 0984 49 20 44. E-mail: f.neve@unical.it.
† Università della Calabria.
‡ Università di Ancona.

(1) Cao, G.; Hong, H.-G.; Mallouk, T. E. *Acc. Chem. Res.* **1992**, *25*, 420.
(2) Thompson, M. E. *Chem. Mater.* **1994**, *6*, 1168.
(3) Almeida, O. J.; Dixon, B. G. *Chem. Mater.* **1995**, *7*, 2039.
(4) Alberti, G.; Casciola, M.; Costantino, U.; Vivani, R. *Adv. Mater.* **1996**, *8*, 291.
(5) Gao, W.; Dickinson, L.; Morin, F. G.; Reven, L. *Chem. Mater.* **1997**, *9*, 3113.
(6) Kimizuka, N.; Kunitake, T. *Adv. Mater.* **1996**, *8*, 89.
(7) Jiang, T.; Ozin, G. A. *J. Mater. Chem.* **1997**, *7*, 2213.
(8) Era, M.; Hattori, T.; Taira, T.; Tsutsui, T. *Chem. Mater.* **1997**, *9*, 8.
(9) Mitzi, D. B.; Wang, S.; Feild, C. A.; Chess, C. A.; Guloy, A. M. *Science* **1995**, *267*, 1473.
(10) Mitzi, D. B. *Chem. Mater.* **1996**, *8*, 791.
(11) Mitzi, D. B.; Liang, K. *Chem. Mater.* **1997**, *9*, 2990.
(12) Bonhomme, F.; Kanatzidis, M. G. *Chem. Mater.* **1998**, *10*, 1153.
(13) Tang, Z.; Litvinchuk, A. P.; Lee, H.-G.; Guloy, A. M. *Inorg. Chem.* **1998**, *37*, 4752.
(14) Oliver, S. R. J.; Lough, A. J.; Ozin, G. A. *Inorg. Chem.* **1998**, *37*, 5021.
(15) Choy, J.-H.; Kwon, S.-J.; Park, G.-S. *Science* **1998**, *280*, 1589.
(16) Choy, J.-H.; Kwon, S.-J.; Hwang, S.-J.; Kim, Y.-I.; Lee, W. *J. Mater. Chem.* **1999**, *9*, 129.
(17) Neve, F.; Crispini, A.; Armentano, S.; Francescangeli, O. *Chem. Mater.* **1998**, *10*, 1904.
(18) Russel, V. A.; Ward, M. D. *J. Mater. Chem.* **1997**, *7*, 1123.
(19) Ward, M. D. *Chem. Br.* **1998**, *34* (9), 52.

10.1021/ic9906959 CCC: $19.00
Published on Web 03/02/2000

Table 1. Crystallographic Parameters, Collection Data, and Refinement Results for $[C14\text{-}Py]_2[PdI_4]$, $[C14\text{-}Py]_2[Pd_2I_6]$, and $[C16\text{-}Py]_2[Pd_2I_6]$

	$[C14\text{-}Py]_2[PdI_4]$	$[C14\text{-}Py]_2[Pd_2I_6]$	$[C16\text{-}Py]_2[Pd_2I_6]$
empirical formula	$C_{38}H_{68}N_2I_4Pd$	$C_{38}H_{68}N_2I_6Pd_2$	$C_{42}H_{72}N_2I_6Pd_2$
fw	1166.9	1527.1	1579.2
space group	$P\bar{1}$	$P\bar{1}$	$P\bar{1}$
a, Å	8.918(3)	9.399(4)	9.417(2)
b, Å	9.894(3)	14.264(6)	14.215(3)
c, Å	29.062(12)	29.415(13)	31.552(6)
α (deg)	93.51(3)	92.11(4)	87.96(3)
β (deg)	94.17(3)	90.07(4)	87.63(3)
γ (deg)	115.60(3)	104.53(3)	75.67(3)
V, Å3	2294(2)	3815(3)	4087(1)
Z	2	3	3
wavelength, Å	0.71073	0.71073	0.71073
temp, K	298	298	298
D_{calc}, g/cm^3	1.689	1.994	1.925
μ (Mo Kα), cm^{-1}	31.121	43.74	40.86
scan type	ω	ω	ω
no. of data collected	7222[R(int) = 0.036]	10029[R(int) = 0.063]	8833[R(int) = 0.057]
no. of observed data	4721 [$I > 2\sigma(I)$]	4897 [$I > 2\sigma(I)$]	5279 [$I > 2\sigma(I)$]
no. of refined params	406	649	703
R^a	0.0575	0.0617	0.0451
R' [b,c]	0.0612[b]	0.0660[b]	0.0984[c]
goodness-of-fit	1.26	0.91	0.93 (on F_o^2)

[a] $R = \sum||F_o| - |F_c||/\sum|F_o|$. [b] $R' = [\sum w(|F_o| - |F_c|)^2/\sum w|F_o|^2]^{1/2}$. [c] $R' = [\sum w(F_o^2 - F_c^2)^2/\sum w(F_o^2)^2]^{1/2}$.

state preorganization built on directional forces and van der Waals interactions. More important, compounds **1** and **2** behaved similarly except for the occurrence of a crystal smectic phase that preceded the mesophase in the case of **1**. We attributed this difference (with respect to 2) to the presence of stronger C−H···X hydrogen bonds[20] and, to a lesser degree, to size effects of the $[PdX_4]^{2-}$ anion.

Here, we present an extension of previous work to include derivatives of the $[PdI_4]^{2-}$ anion. $[Cn\text{-}Py]_2[PdI_4]$ (**3**, n = 14, 16), which were obtained starting from a 2:1 ratio of the organic cation to "PdI_2", represent new phases with a crystalline bilayer-type architecture (layering motif **B** in Chart 1). Variation of the above experimental ratio to 1:1 resulted in the formation of the phases $[Cn\text{-}Py]_2[Pd_2I_6]$ (**4**, n = 14, 16), which were shown to consist of interdigitated cations segregated between anionic layers of individual $[Pd_2I_6]^{2-}$ spacers. Evidence for the mesomorphic behavior of **3**(n = 16) is also given.

Experimental Section

Instrumentation. C, H, and N analyses were carried out with a Perkin-Elmer 2400 microanalyzer. NMR spectra were recorded with a Bruker AC 300. Optical observations were carried out with a Zeiss Axioskop polarizing microscope equipped with a Linkam CO 600 heating stage and a temperature control unit. Phase transition temperatures were measured by differential scanning calorimetry (DSC) with a Perkin-Elmer DSC-7 instrument [scanning rate 5 °C/min; transition temperatures taken as a peak top]. Variable-temperature powder X-ray diffraction (VT-PXRD) measurements were performed with an INEL CPS 120 powder diffractometer [Cu Kα radiation, λ = 1.54056 Å]. Indexing of the powder patterns was performed using the Cerius[2] program.[21] X-ray diffraction data on single crystals were collected on a Siemens R3m/V four-circle diffractometer with graphite-monochromated Mo Kα radiation (λ = 0.71073 Å).

Materials. $PdCl_2$ and potassium iodide were used as received from Aldrich. The *N*-alkylpyridinium iodide precursors $[Cn\text{-}Py][I]\cdot H_2O$ (n = 14, 16) were obtained from the bromide analogues[17] by reaction with potassium iodide[22] and recrystallization from a pyridine/diethyl ether mixture. $[Cn\text{-}Py][I]\cdot H_2O$ show a single thermotropic lamellar phase in the ranges 99.0−208.3 °C (n = 16) and 95.4−159.3 °C (n = 14).

Syntheses. $[Cn\text{-}Py]_2[PdI_4]$ (**3**; n = 14, 16). The two salts **3** (n = 14, 16) were prepared following the same procedure. A solution of $PdCl_2$ (0.05 g, 0.28 mmol) in acetonitrile (15 mL) was treated with a saturated aqueous solution (2 mL) of excess KI (10 equiv), and the resulting dark solution was filtered through a glass frit. Then, 2 equiv of pyridinium iodide $[Cn\text{-}Py][I]\cdot H_2O$ was added to the filtrate and the solution heated to 60−70 °C for ca. 30 min. Precipitation of a dark brown microcrystalline product was achieved directly from the reaction mixture (n = 16) or upon cooling of the solution to −18 °C (n = 14). The solid was usually washed with water, small amounts of acetone, and diethyl ether and vacuum-dried. The absence of cocrystallized solvent was confirmed by ^{1}H NMR spectroscopy.

3(n = 16): yield, 95%. Anal. Calcd for $C_{42}H_{76}I_4N_2Pd$: C, 41.24; H, 6.26; N, 2.29. Found: C, 40.95; H, 6.19; N, 2.40.

3(n = 14): yield, 98%. Anal. Calcd for $C_{38}H_{68}I_4N_2Pd$: C, 39.11; H, 5.87; N, 2.40. Found: C, 39.25; H, 5.90; N, 2.58.

$[Cn\text{-}Py]_2[Pd_2I_6]$ (4; n = 14, 16). The salts 4 (n = 14, 16) were obtained as compounds **3** by means of a 1:1 molar ratio of "PdI_2" (prepared in situ) and $[Cn\text{-}Py][I]\cdot H_2O$. The reaction mixture was heated to reflux for 2 h. Overnight cooling of the resulting dark solution afforded the product as black, long needles. While for **4**(n = 16) the solid obtained from the reaction mixture was analytically pure, for **4**(n = 14) the final purity was achieved upon recrystallization from an acetonitrile/diethyl ether mixture at −18 °C to eliminate trace amounts of **3**(n = 14).

4(n = 16): yield, 86%. Anal. Calcd for $C_{42}H_{76}I_6N_2Pd_2$: C, 31.88; H, 4.84; N, 1.77. Found: C, 31.88; H, 4.88; N, 1.74.

4(n = 14): yield, 87%. Anal. Calcd for $C_{38}H_{68}I_6N_2Pd_2$: C, 29.89; H, 4.49; N, 1.83. Found: C, 29.88; H, 4.40; N, 1.83.

Crystal Structure Determination of 3(n = 14) and 4(n = 14, 16). Brown needlelike crystals of $[C14\text{-}Py]_2[PdI_4]$, **3**(n = 14), crystallized at − 18 °C from the reaction mixture. The crystals were aggregates of light brown plates, one of which was used for data collection. Black needles of both $[C14\text{-}Py]_2[Pd_2I_6]$, **4**($n$ = 14) and $[C16\text{-}Py]_2[Pd_2I_6]$, **4**($n$ = 16), crystallized from an acetonitrile/diethyl ether mixture at −18 °C. Smaller specimens were obtained upon cutting larger needles. Single-crystal data of **3**(n = 14) and **4**(n = 14, 16) with details of the structure solution and refinement are summarized in Table 1. The data were corrected for Lorentz, polarization, and X-ray absorption effects. An empirical absorption correction was applied using a method based

(20) Aakeröy, C. B.; Seddon, K. R. *Chem. Soc. Rev.* **1993**, 397.
(21) *CERIUS^2 3.0 Molecular Simulations Program*; Molecular Simulations Inc.: San Diego, CA.
(22) Navarro-Rodriguez, D.; Frere, Y.; Gramain, P.; Guillon, D.; Skoulios, A.; Nicoud, J. F. *Liq. Cryst.* **1991**, *9*, 321.

upon azimuthal Ψ scan data.[23] The structures of $[C14\text{-}Py]_2[PdI_4]$ and $[C14\text{-}Py]_2[Pd_2I_6]$ were solved with the SHELXTL PLUS package[24] and refined by full-matrix least-squares refinement on *F*. The structure of $[C16\text{-}Py]_2[Pd_2I_6]$ was solved with the SHELXTL PLUS package and refined with SHELX93[25] by full-matrix least-squares refinement on F_2 using all data. All the non-hydrogen atoms were refined anisotropically, and the hydrogen atoms were included in calculated positions and treated as riding atoms. The isotropic displacement parameter of each hydrogen atom was fixed at $U = 0.08$ Å^2. Some of the geometrical calculations have been performed with the PARST program.[26]

Results and Discussion

***N*-Alkylpyridinium Tetraiodopalladate, $[Cn\text{-}Py]_2[PdI_4]$.** The compounds $[Cn\text{-}Py]_2[PdI_4]$ (**3**; $n = 14$, 16) were prepared from mesomorphic *N*-alkylpyridinium salts [C*n*-Py][I] and "PdI_2" (prepared in situ from $PdCl_2$ and excess potassium iodide) in a straightforward manner and crystallized as lancelets or plates directly from the reaction mixture.

Compounds **3** were investigated for thermotropic mesomorphism by thermal polarizing optical microscopy, differential scanning calorimetry (DSC), and diffractometric techniques. Both optical microscopy and DSC observations showed that while **3**($n = 14$) melts to an isotropic liquid at 100.6 °C ($\Delta H =$ 86.8 kJ mol^{-1}), **3**($n = 16$) undergoes a reversible melting to a mesophase at 106.0 °C ($\Delta H = 99.9$ kJ mol^{-1}), followed by clearing to the isotropic liquid phase at 138.0 °C ($\Delta H = 0.6$ kJ mol^{-1}). The optical texture of the mesophase of **3**($n = 16$) produced by slow cooling from the isotropic phase appears between crossed polarizers as dimly birefringent oily streaks interspersed with much larger regions of uniform extinction (homeotropic regions). The first DSC run also features a crystal-to-crystal transition at 89.1 °C with a relatively small enthalpic content ($\Delta H = 6.7$ kJ mol^{-1}), and which is not observed in subsequent runs.

The polymorphism of **3**($n = 16$) was confirmed by variable-temperature powder X-ray diffraction (VT-PXRD). The powder patterns at different temperatures are shown in Figure 1. The room-temperature crystal phase shows a lamellar structure (we observe 3 orders of reflections) with a repeating layer distance *d* of 31.70 Å. At ≈90 °C a crystal-to-crystal phase transition occurs in which the lamellar structure is retained with a periodicity of 31.28 Å. Both the crystal phases shown by a pristine sample of **3**($n = 16$) can be indexed in the triclinic crystal system. Cell parameters for the room-temperature crystal phase of **3**($n = 16$) are $a = 8.137(1)$ Å, $b = 9.135(1)$ Å, $c =$ 31.841(5) Å; $\alpha = 90.7(1)°$, $\beta = 91.5(1)°$, $\gamma = 105.2(1)°$, $V =$ 2193.8 Å^3. The corresponding cell parameters for the high-temperature crystal phase at 95 °C are $a = 8.682(1)$ Å, $b =$ 9.807(1) Å, $c = 31.480(3)$ Å; $\alpha = 83.58(1)°$, $\beta = 87.70(2)°$, γ $= 64.78(3)°$, $V = 2409.5$ Å^3.

The VT-PXRD pattern also shows that the melting transition at 106.0 °C leads to a smectic phase with disordered, liquidlike alkyl chains (Figure 1, upper trace). The d_{001} spacing of **3**($n =$ 16) in the liquid crystal phase (32.3 Å) points to a quasi-single-layered smectic A phase with strong interdigitation of chains. This assignment is strongly supported by the characteristic optical textures[27,28] observed under crossed polarizers. Further support stems from the very low ΔH value at the clearing point.

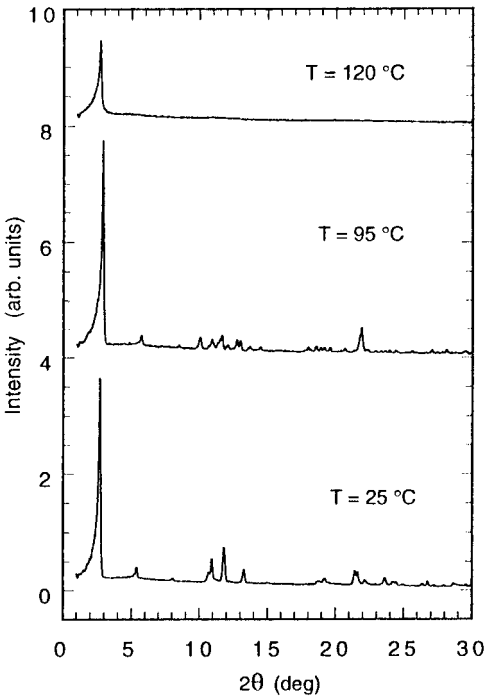

Figure 1. Variable-temperature powder XRD patterns of $[C16\text{-}Py]_2[PdI_4]$, **3**($n = 16$), in the first heating cycle.

Crystal Structure of $[C14\text{-}Py]_2[PdI_4]$, 3($n = 14$). Brown single crystals of **3**($n = 14$) grown directly from the reaction mixture were found suitable for an X-ray diffraction study. A view of the asymmetric unit is shown in Figure 2.

In the asymmetric unit the organic cations are arranged with straight hydrocarbon chains running parallel to each other in an overall head-to-head fashion (Figure 2). The mean coordination plane of the $[PdI_4]^{2-}$ anion is nearly orthogonal to both the mean planes of the pyridine rings (dihedral angles of 70° and 83°, respectively). The bond lengths, bond angles, and average torsion angles of the hydrocarbon chains (trans-planar conformation) are found to be similar to those observed in the related salts $[Cn\text{-}Py]_2[PdX_4]$ (X = Cl, Br)[17] and other pyridinium salts.[29−31] The geometry around the Pd atom in the $[PdI_4]^{2-}$ anion is slightly distorted square-planar (Figure 2). To the best of our knowledge, no other examples of crystallographically characterized tetraiodopalladate species are available for comparison. Nevertheless, the Pd−I distances are within the range of values for terminal Pd−I bonds [2.409−2.811 Å] obtained through the analysis of 62 structures containing the fragment PdI2 and recorded in the Cambridge Structural Database (CSD).[32]

In 3-D space, the salt **3**($n = 14$) gives rise to an interdigitated bilayer packing arrangement with a basal spacing of 29.0 Å, in which the hydrocarbon chains of the cations run almost parallel to the [001] direction (Figure 3). A mere canting of 8° of the alkyl chains with respect to the stacking planes is observed. The polar region, which roughly spans 10 Å, contains two symmetrical rows of alternating anions and pyridinium headgroups. The repetition motif along the *b* axis is such that two

(23) North, A. C. T.; Phillips, D. C. *Acta Crystallogr., Sect. A* **1968**, *24*, 351.
(24) *SHELXTL PLUS*, version 4.21; Siemens Analytical X-ray Instruments Inc.: Madison, WI, 1990.
(25) Sheldrick, G. M. *SHELXL93: Program for the Refinement of Crystal Structures*; University of Göttingen: Göttingen, Germany, 1993.
(26) Nardelli, M. *Comput. Chem.* **1983**, *7*, 95.
(27) Demus, D.; Richter, L. *Textures of Liquid Crystals*; Verlag Chemie: Weinheim, 1978.
(28) Bouligand, Y. In *Handbook of Liquid Crystals, Vol.1: Fundamentals*; Demus, D., Gray, G. W., Spiess, H.-W., Vill, V., Eds.; Wiley-VCH: Weinheim, 1998.
(29) Paradies, H. H.; Habben, F. *Acta Crystallogr.* **1993**, *C49*, 744.
(30) Virovets, A. V.; Vakulenko, N. N.; Volkov, V. Podberezkaya, N. V. *Zh. Strukt. Khim.* **1994**, *35*, 72.
(31) Vongbupnimit, K.; Noguchi, K.; Okuyama, K. *Acta Crystallogr.* **1995**, *C51*, 1940.
(32) Allen, F. H.; Kennard, O. *Chem. Des. Autom. News* **1993**, *8*, 31.

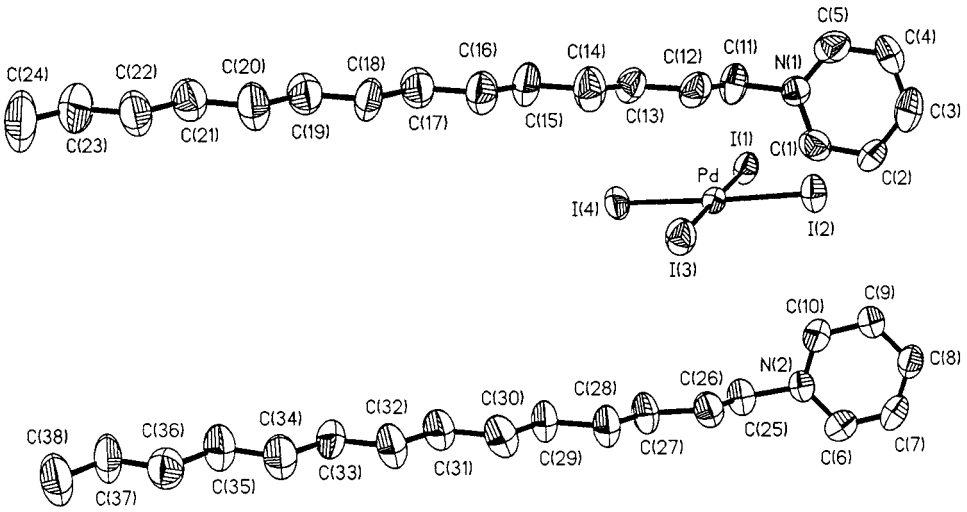

Figure 2. Thermal ellipsoids and numbering scheme of the asymmetric unit of $[C14\text{-}Py]_2[PdI_4]$, **3**($n = 14$). Relevant metric parameters (distances, Å; angles, deg): Pd−I(1) 2.625(2), Pd−I(2) 2.622(2), Pd−I(3) 2.615(2), Pd−I(4) 2.629(2); I(1)−Pd−I(2) 89.2(1), I(1)−Pd−I(3) 178.8(1), I(2)−Pd−I(3) 90.0(1), I(1)−Pd−I(4) 90.6(1), I(2)−Pd−I(4), 177.5(1), I(3)−Pd−I(4) 90.3(1)°.

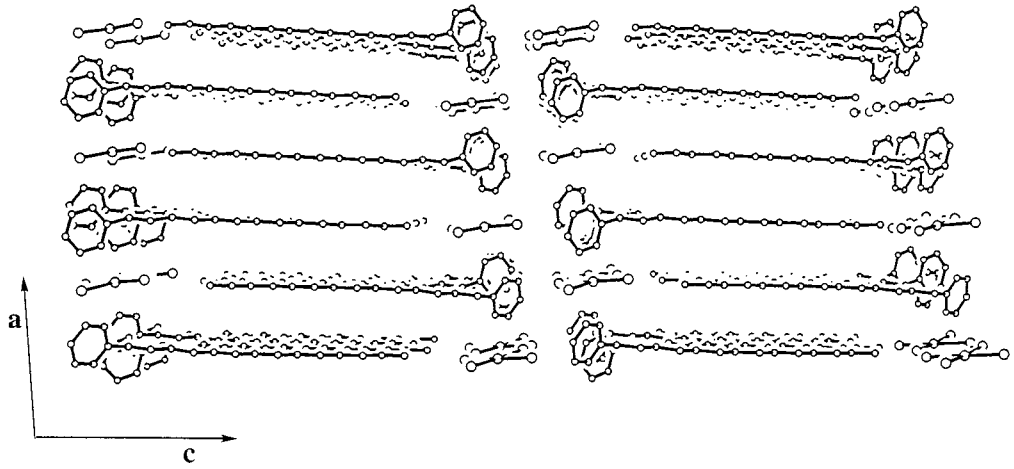

Figure 3. Crystal packing of $[C14\text{-}Py]_2[PdI_4]$, **3**($n = 14$), viewed along the *b*-axis.

pyridine rings are interleaved between two $[PdI_4]^{2-}$ anions with a mean transverse shift of 3.41 Å with respect to the palladium centers.

Although single-crystal data for the entire series $[C14\text{-}Py]_2[PdX_4]$ (X = Cl, Br, I) are not available, it is instructive to note the occurrence of an interdigitated bilayer structure in $[C14\text{-}Py]_2[PdI_4]$ compared to the stacked single-layer motif observed for the complex salts $[C16\text{-}Py]_2[PdX_4]$ (X = Cl, Br).[17] To make the comparison more sound, it is important to recall that the unit cell dimensions of $[C16\text{-}Py]_2[PdI_4]$ obtained from X-ray powder diffraction point to the same structure as for the lower homologue ($n = 14$) with the major difference being the increased value of the c parameter as would be expected for an isostructural lamellar solid built on a longer chain cation. In our opinion, the striking difference in structural motifs between the iodo species, on one side and the chloro and bromo analogues, on the other, resides in the mutual disposition of the cations within the asymmetric unit. In fact, since the palladium atom of the $[PdX_4]^{2-}$ anion lies on the inversion center, in both compounds $[C16\text{-}Py]_2[PdCl_4]$ and $[C16\text{-}Py]_2[PdBr_4]$ the number of molecules in the asymmetric unit (Z') is 0.5.[17] Therefore, the aliphatic chains of the pyridinium cations point to opposite sides of the $[PdX_4]^{2-}$ anions with the pyridine rings stacked to each other. The large values of the interplanar distances and offsets along the ± *x*-axis (e.g., 4.55 and 7.32 Å, respectively, for compound $[C16\text{-}Py]_2[PdCl_4]$) are in agreement with the presence of the $[PdX_4]^{2-}$ anion sandwiched between the two pyridine rings. This arrangement appears to be the only one consistent with the generation of an interdigitated single-layer packing. On the other hand, the replacement of the halogen atoms in $[PdX_4]^{2-}$ (X = Cl, Br) for iodine atoms, first of all, causes a change in the value of Z' from 0.5 to 1 (observed for $[C14\text{-}Py]_2[PdI_4]$ and calculated in the case of $[C16\text{-}Py]_2[PdI_4]$). In addition, both a change of the orientation of the aliphatic chains of the cations from anti to syn and a loss of stacking between the pyridine rings occur. With respect to the latter point, and although the interplanar angle is 16°, the interplanar distance and the offset at 1.92 and 3.11 Å, respectively, for $[C14\text{-}Py]_2[PdI_4]$ clearly indicate a strong tendency toward coplanarity of the two mean planes (Figure 2).

All of the above changes, which necessarily lead to different crystal packings on going from compounds $[C16\text{-}Py]_2[PdCl_4]$ and $[C16\text{-}Py]_2[PdBr_4]$ to $[C14\text{-}Py]_2[PdI_4]$, can be ascribed to both the difference in the steric demand of the anion and the nature and strength of the interionic interactions. It has been previously shown[17] that in both crystalline $[C16\text{-}Py]_2[PdCl_4]$ and $[C16\text{-}Py]_2[PdBr_4]$ all the halogen atoms of the anion, within the ionic sublayer, participate in H···X contacts with the hydrogen atoms of the pyridinium ring cations, which are significantly shorter than the sum of the van der Waals radii of

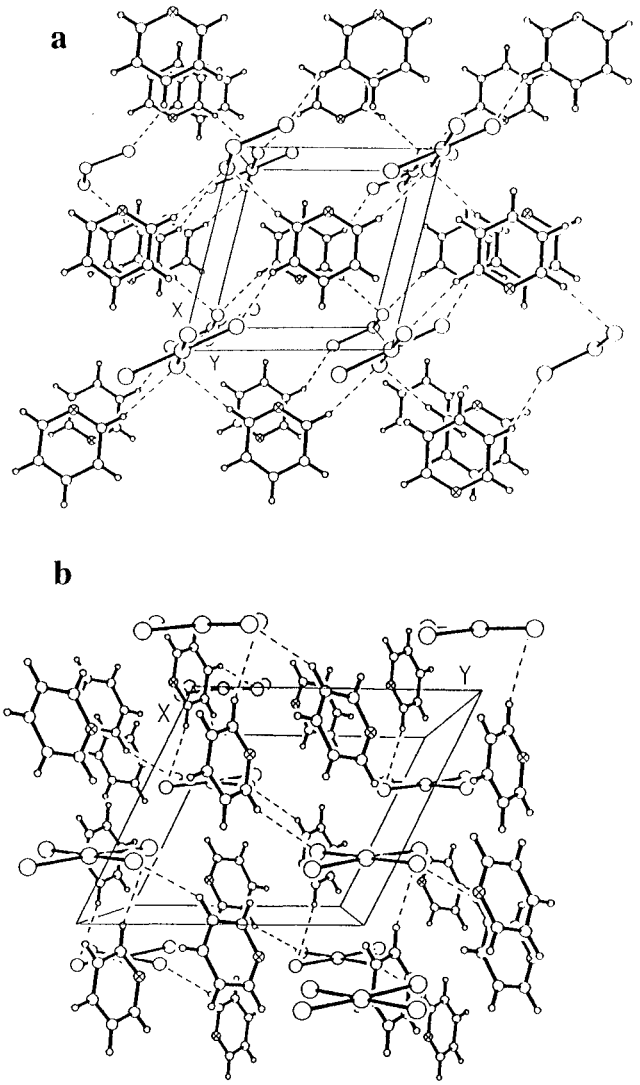

Figure 4. Ball and stick representation showing the C−H···X intermolecular contacts in the *ab* plane for (a) [C16-Py]$_2$[PdCl4] (see ref 10 for details) and (b) [C14-Py]$_2$[PdI$_4$], **3**(n = 14), with aliphatic chains omitted for clarity. Hydrogen-bonding contacts (Å) (symmetry codes in parentheses) for **3**(n = 14): I(1)···H(2a) (x, y − 1, z) 3.02(1), I(3)···H(10), 3.13(1), I(4)···H(6b) (1 − x, 1 − y, z) 3.03(1).

hydrogen and chlorine or bromine, respectively (Figure 4a). The crystallographic evidence (C−H···X and C···X distances, C−H···X angles) coupled to the results of charge distribution calculations (CNDO/2, INDO, and MNDO) on an isolated pyridinium cation showing the existence of a reasonable $\delta(+)$ charge of the C−H ring protons[20,33] allows us to debate the existence of two-dimensional hydrogen-bond networks in the *ab* plane. The significance of the C−H···X hydrogen-bond-like interactions to the organization of the solid state in these systems appears more evident with the substitution of the hydrogen-bond acceptor, i.e., the halogen atom X in the $[PdX_4]^{2-}$ anion. In the crystal structure of [C14-Py]$_2$[PdI$_4$] there are few C−H···I contacts shorter than 3.18 Å (the sum of the van der Waals radii of hydrogen and iodine atoms[34]) which can hardly be considered as hydrogen bonds[35] (Figure 4b). Therefore, the formation of relatively strong (X = Cl, Br) or very weak (X = I) C−H···X hydrogen bonds in the $[PdX_4]^{2-}$ pyridinium salts, which is a complex result of electrostatic and polarization effects, is partially responsible for (i) the differences in their physical properties (thermotropic behavior) and (ii) the arrangement of the molecules in the solid state. Nevertheless, in the absence of a correct estimate of the hydrogen-bond contributions to the total lattice energy,[20] a structure−property correlation for the present systems should be considered only as a qualitative one.

***N*-Alkylpyridinium Hexaiododipalladate, [C*n*-Py]$_2$[Pd$_2$I$_6$].** Several attempts were made to grow single crystals of **3**(n = 16). The best results were obtained when acetonitrile/diethyl ether was used as the recrystallization medium. Thus, large black needles formed at −18 °C, but turned out to be different in composition with respect to the starting solid material. Yet, such a crystalline solid had no thermotropic mesomorphic behavior and it analyzed for a species which apparently contained $[Pd_2I_6]^{2-}$ anions and *N*-alkylpyridinium cations in a 1:2 ratio. Additionally, the formation of such a species could be completely avoided when the recrystallization took place in the presence of a 10-fold excess of potassium iodide (dissolved in a few drops of water). A lower excess of KI invariably resulted in the formation of a mixture of crystals of **3**(n = 16) and the newly formed species. Puzzled by these results, and by the fact that **3**(n = 14) did seem to remain unaffected under the same experimental conditions, we attempted to prepare this somewhat unexpected[36] species in a less serendipitous manner.

[C*n*-Py]$_2$[Pd$_2$I$_6$] (**4**) was successfully prepared for n = 14 and 16 by reaction of "PdI$_2$" and the pyridinium cation in a 1:1 molar ratio. Complex salt **4** indeed crystallized as well-formed black needles from a cold acetonitrile/diethyl ether mixture. Single crystals were obtained for both **4**(n = 14) and **4**(n = 16). Single-crystal XRD analysis showed that the two homologues are isostructural with a longer *c*-axis for complex **4**(n = 16) (Table 1), which reasonably matches the lengthening of the aliphatic chains. Since in both cases (n = 14 and 16) one of the two independent $[Pd_2I_6]^{2-}$ anions in the asymmetric unit lies on a crystallographic inversion center, three independent alkylpyridinium cations are found with the aliphatic chains in a parallel orientation. Figure 5 shows a view of the asymmetric unit for **4**(n = 14). The coordination around the palladium atoms in the $[Pd_2I_6]^{2-}$ anions is distorted square-planar, due to the presence of bridging iodine atoms (Table 2). No remarkable difference is found between the Pd−I bridging distances [mean values of 2.620 and 2.612 Å respectively for **4**(n = 14) and **4**(n = 16)] and the terminal ones [mean values of 2.601 and 2.605 Å respectively for **4**(n = 14) and **4**(n = 16)]. These values, as well as the Pd···Pd intraionic distances [(3.859(1) and 3.829(1) Å for **4**(n = 14), 3.855(2) and 3.822(1) Å for **4**(n = 16)], are similar to those previously observed for isoquinolinium[37,38] and tetra-*n*-butylammonium[39] salts containing the $[Pd_2I_6]^{2-}$ anion.

On going from $[PdI_4]^{2-}$ to $[Pd_2I_6]^{2-}$ a drastic change occurs in terms of mutual disposition of anions and cations in compound **4** with respect to **3**. The number of molecules in the asymmetric unit of **4** is 1.5 in both cases (n = 14 and 16), with

(33) Lubkowski, J.; Blazejowski, J. *J. Phys. Chem.* **1991**, *95*, 2311.
(34) Bondi, A. *J. Phys. Chem.* **1964**, *68*, 441.
(35) A.-Sada, A. K.; Greenway, A. M.; Hitchcock, P. B.; Mohammed, T. J.; Seddon, K. R.; Zora, J. A. *J. Chem. Soc., Chem. Commun.* **1986**, 1753.
(36) For a report about the formation of $[M_2X_6]^{2-}$ (M = Pd, Pt) anions from solutions of the corresponding $[MX_4]^{2-}$ ions, see: Harris, C. M.; Livingstone, S. E.; Stephenson, N. C. *J. Chem. Soc.* **1958**, 3697.
(37) Maassarani, F.; Pfeffer, M.; Le Borgne, G. *J. Chem. Soc., Chem. Commun.* **1987**, 565.
(38) Maassarani, F.; Pfeffer, M.; Le Borgne, G. *Organometallics* **1987**, *6*, 2043.
(39) Chan, S.; Lee, S.-M.; Lin, Z.; Wong, W.-T. *J. Organomet. Chem.* **1996**, *510*, 219.

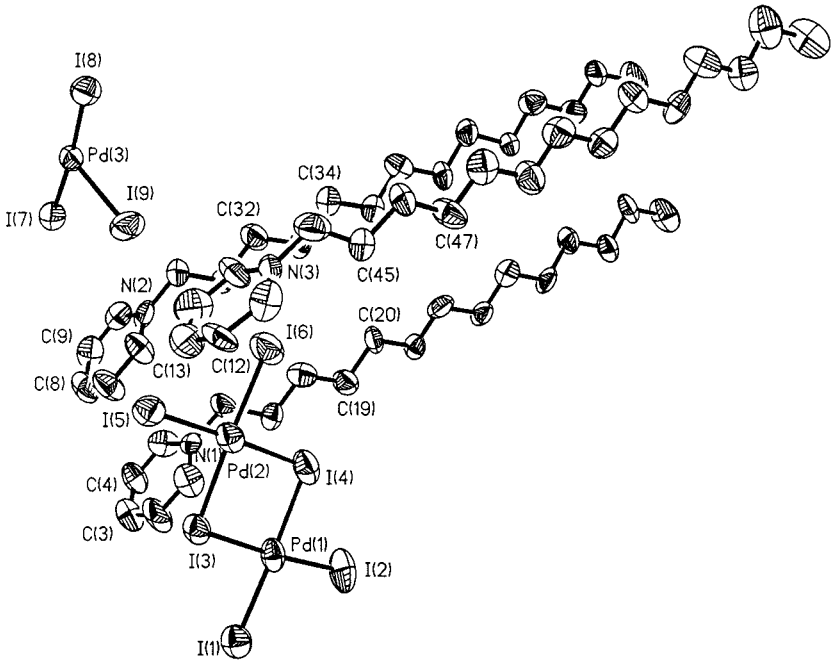

Figure 5. Thermal ellipsoids and atomic numbering scheme of the asymmetric unit of $[C14\text{-}Py]_2[Pd_2I_6]$, **4**($n = 14$).

Table 2. Selected Bond Lengths (Å) and Angles (deg) for $[C14\text{-}Py]_2[Pd_2I_6]$ and $[C16\text{-}Py]_2[Pd_2I_6]$

	$[C14\text{-}Py]_2[Pd_2I_6]$	$[C16\text{-}Py]_2[Pd_2I_6]$
Pd(1)−I(1)	2.614(3)	2.576(2)
Pd(1)−I(2)	2.578(3)	2.609(2)
Pd(1)−I(3)	2.631(3)	2.615(2)
Pd(1)−I(4)	2.616(3)	2.628(2)
Pd(2)−I(3)	2.635(3)	2.599(2)
Pd(2)−I(4)	2.614(3)	2.611(2)
Pd(2)−I(5)	2.618(3)	2.612(2)
Pd(2)−I(6)	2.595(3)	2.633(2)
Pd(3)−I(7)	2.606(3)	2.599(2)
Pd(3)−I(8)	2.618(3)	2.601(2)
Pd(3)−I(9)	2.597(3)	2.607(2)
Pd(3)−I(8a)	2.604(3)	2.614(2)
I(1)−Pd(1)−I(2)	91.3(1)	91.43(6)
I(1)−Pd(1)−I(3)	92.8(1)	90.32(6)
I(2)−Pd(1)−I(3)	174.2(1)	177.99(6)
I(1)−Pd(1)−I(4)	178.0(1)	174.00(6)
I(2)−Pd(1)−I(4)	90.4(1)	92.85(5)
I(3)−Pd(1)−I(4)	85.3(1)	85.33(5)
I(3)−Pd(2)−I(4)	85.3(1)	85.31(6)
I(3)−Pd(2)−I(5)	91.8(1)	90.48(6)
I(4)−Pd(2)−I(5)	177.1(1)	175.09(6)
I(3)−Pd(2)−I(6)	175.2(1)	177.19(6)
I(4)−Pd(2)−I(6)	90.6(1)	91.91(5)
I(5)−Pd(2)−I(6)	92.3(1)	92.28(6)
I(7)−Pd(3)−I(8)	175.4(1)	176.80(6)
I(7)−Pd(3)−I(9)	93.2(1)	93.25(6)
I(8)−Pd(3)−I(9)	91.3(1)	89.68(5)
I(7)−Pd(3)−I(8a)	89.8(1)	91.17(5)
I(8)−Pd(3)−I(8a)	85.7(1)	85.88(5)
I(9)−Pd(3)−I(8a)	176.8(1)	175.49(5)

one of the two $[Pd_2I_6]^{2-}$ anions lying astride an inversion center. The molecular arrangement which takes place in the crystal is a compromise between an interdigitated single-layer and a bilayer packing mode. Figure 6 shows the crystal packing for **4**($n = 14$). We can ideally look at the crystal packing of these systems as a combination of two different sublattices: one arising from the centrosymmetrical part of the asymmetric unit (Figure 6, top view) and a second one from the remaining part (Figure 6, middle view). In the single-layer sublattice (Figure 6, top view) the $[Pd_2I_6]^{2-}$ anion is sandwiched between two pyridine rings [at a dihedral angle of 113.7(2)° for **4**($n = 14$) and 114.4(3)° for **4**($n = 16$)]. The large value of the interplanar distance between the pyridine rings at 9.62 Å (12.93 Å is the corresponding value for **4**($n = 16$)) takes into account the presence of a rather large anion between them. This sublattice motif is comparable to the layering modes found for $[CTA]_2[Zn_2Cl_6]$ (CTA = cetyltrimethylammonium)[40] and $[DDA]_4[Sn_2S_6]$ (DDA = dodecylammonium)[41] where the anion also lies on an inversion center. The polar region of the bilayer sublattice (Figure 6, middle view) along the *a*-direction contains two rows of pyridinium headgroups, while two rows of anions run above and below it. As it is shown in Figure 6 (bottom view), which shows the complete crystal packing for compound **4**($n = 14$), the empty space between the two rows of pyridinium headgroups is filled with the third row of $[Pd_2I_6]^{2-}$ anions (the centrosymmetrical ones). The mean planes of the anions belonging to the central row are mutually perpendicular to the corresponding planes of neighboring anions (dihedral angles of 80.2° and 80.6° for **4**($n = 14$) and **4**($n = 16$), respectively).

The aliphatic chains of **4** are found to be highly interdigitated and relatively tilted with respect to the layer normal at a mean angle of 29° for **4**($n = 14$) and 27° for **4**($n = 16$). The corresponding interlayer distances are 29.4 and 31.5 Å, respectively.

The search for significant H···I contacts in **4** gave a very small number of results approaching the threshold value of 3.18 Å.[34] **4**($n = 14$) shows only one short contact [I(5)···H(10), 2.94(2) Å], whereas **4**($n = 16$) has two longer contacts [I(2)···H(4) ($x - 1, y, z$), 3.11(2) Å; I(6)···H(6) ($x + 1, y, z$), 3.12(1) Å]. Although no tight correlation can be made, the reduced importance of hydrogen-bonding interactions in complex salts **4** with respect to **3** (wherein it is already rather low) is mirrored by the disappearance of any mesomorphic behavior. Compound **4**($n = 14$) melts to an isotropic liquid at 73.6 °C with a ΔH value of 25.1 kJ mol^{-1}. Slightly higher values for these parameters (82.5 °C and 35.5 kJ mol^{-1}, respectively) are

(40) Martin, J. D.; Dattelbaum, A. M.; Thornton, T. A.; Sullivan, R. M.; Yang, J.; Peachey, M. T. *Chem. Mater.* **1998**, *10*, 2699.
(41) Li, J.; Marler, B.; Kessler, H.; Soulard, M.; Kallus, S. *Inorg. Chem.* **1997**, *36*, 4697.

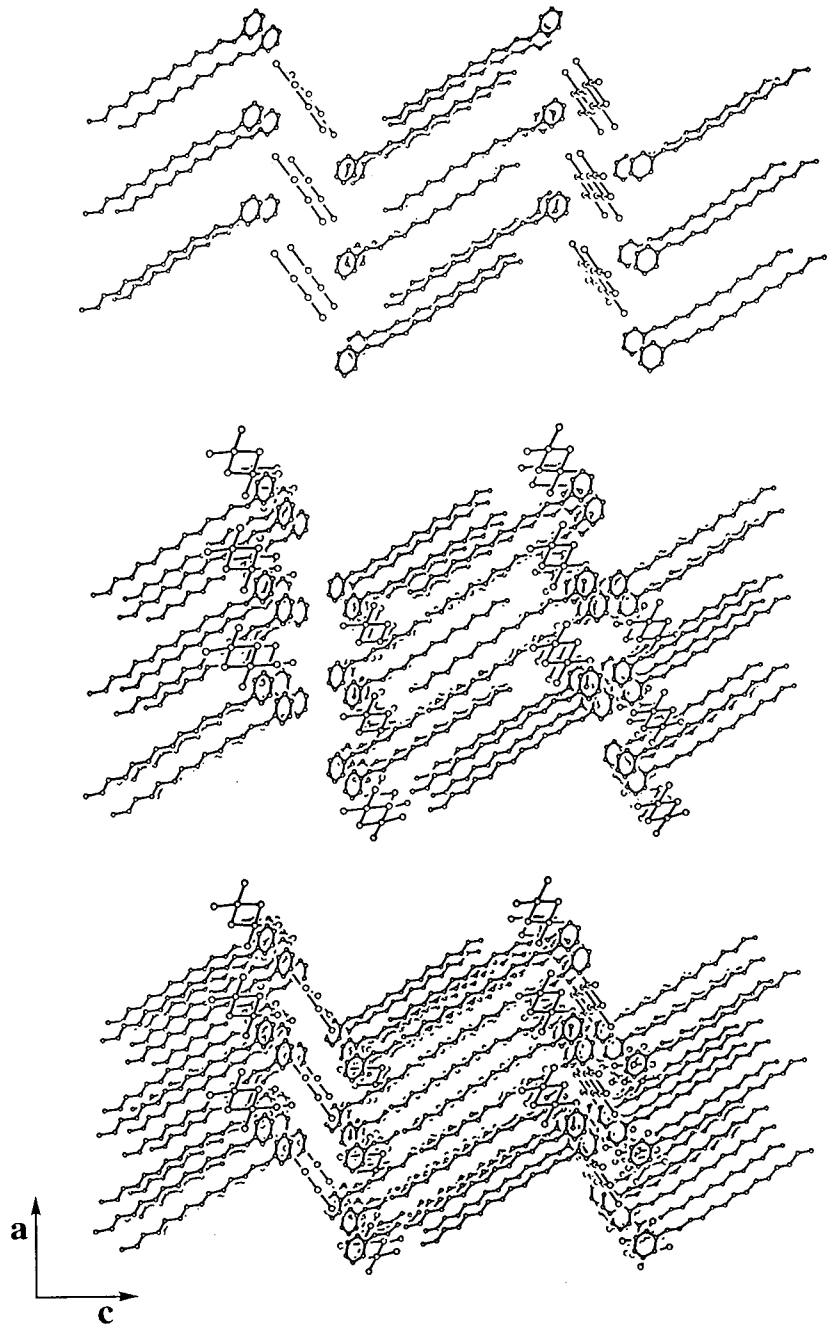

Figure 6. Ball and stick representation of the crystal packing of $[C14\text{-}Py]_2[Pd_2I_6]$, **4**($n = 14$) (bottom view), viewed along the *b*-axis. Separate views show the coexistence of bilayer (middle view) and interdigitated single-layer (top view) sublattices within the crystal packing.

observed for **4**($n = 16$). The lower melting transition temperatures and ΔH values of **4**, as compared to those for **3**, are indicative of a less efficient crystal packing and/or a diminishing strength of secondary, noncovalent forces (hydrogen bonding, chain−chain interactions, etc.).

Conclusions

The control of ordering motifs in lamellar functional materials is a highly desirable goal in view of the exploitation of such materials. Tuning is usually achieved by variation of the molecular components. The organic−inorganic mesoscopic materials $[Cn\text{-}Py]_2[PdI_4]$ and $[Cn\text{-}Py]_2[Pd_2I_6]$ we have prepared seem to be a fine example of control through the inorganic component. Changing the halide of $[PdX_4]^{2-}$ along the series $[Cn\text{-}Py]_2[PdX_4]$ (X = Cl,[17] Br,[17] I) leads to a variation of the layer stacking mode, with the iodopalladate term as the turning point of the series (at least from a structural point of view). On the other hand, the absence of mesomorphism in $[C14\text{-}Py]_2[PdI_4]$ is in line with previous findings on the chloro and bromo analogues.[17] Along the series we observed an enantiotropic mesophase for the chloropalladate with a very narrow range of existence, a monotropic one for the bromopalladate, and no mesophase at all for the iodopalladate salt. Such a trend parallels the decreasing strength of hydrogen-bonding interactions between the $[PdX_4]^{2-}$ anion and the pyridinium cations (i.e., Cl > Br > I). The key role that hydrogen bonding may play in the structural chemistry of smectogenic *N*-alkylpyridinium salts appeared underestimated in previous studies on *N*-alkylpyridinium halides.[22,42] However, the importance of this structural element was pointed out for liquid-crystalline *N*,*N*-dialkylben-

(42) Bazuin, C. G.; Guillon, D.; Skoulios, A.; Nicoud, J. F. *Liq. Cryst.* **1986**, *1*, 181.

zimidazolium halides.[43] Since the occurrence of strong hydrogen bonds involving M−Cl moieties has been recently recognized,[44] it is now important to enlarge the range of metals for which *N*-alkylpyridinium salts of $[MX_4]^{2-}$ (notably $[MCl_4]^{2-}$) form. The goal would be one of approaching, if not matching, the structural diversity observed for other related organic cations.[45−48]

A second result of this study was the preparation of the species $[Cn\text{-}Py]_2[Pd_2I_6]$, where the thermodynamical instability of $[PdI_4]^{2-}$ toward dimerization is likely the driving force of the reaction. However, this instability might be turned into an advantage to prepare new classes of ordered, yet nonmesomorphic, solids. Further, the variation of the cationic molecular component is another possibility to expand the realm of lamellar solids with varying interlayer spacings and related functions.

Acknowledgment. Financial support from the italian Ministero dell'Università e della Ricerca Scientifica e Tecnologica (MURST) and Consiglio Nazionale delle Ricerche (CNR) is gratefully acknowledged. We are indebted to Prof. A. G. Orpen (University of Bristol) for valuable suggestions. Thanks are also expressed to F. Cofone for technical assistance.

Supporting Information Available: X-ray crystallographic files in CIF format for the structural determinations of $[C14\text{-}Py]_2[PdI_4]$, $[C14\text{-}Py]_2[Pd_2I_6]$, and $[C16\text{-}Py]_2[Pd_2I_6]$. This material is available free of charge via the Internet at http://pubs.acs.org.

IC9906959

(43) Lee, K. M.; Lee, C. K.; Lin, I. J. B. *Chem. Commun.* **1997**, 899.
(44) Aullón, G.; Bellamy, D.; Brammer, L.; Bruton, E. A.; Orpen, A. G. *Chem. Commun.* **1998**, 653.
(45) Barbour, L. J.; MacGillivray, L. R.; Atwood, J. L. *Supramol. Chem.* **1996**, *7*, 167.
(46) Lewis, G. R.; Orpen, A. G. *Chem. Commun.* **1998**, 1873.
(47) Guan, J.; Tang, Z.; Guloy, A. M. *Chem. Commun.* **1999**, 1833.
(48) Gillon, A. L.; Orpen, A. G.; Starbuck, J.; Wang, X.-M.; Rodríguez-Martín, Y.; Ruiz-Pérez, C. *Chem. Commun.* **1999**, 2287.